International Journal of Research in Engineering and Science (IJRES)
ISSN (Online): 2320-9364, ISSN (Print): 2320-9356
www.ijres.org Volume 14 Issue 9 ǁ September 2026 ǁ PP. 09-20

An Experimental Study on Combustion Stability and Performance of Biogas Power Generation by Changing Spark Timing

Hsing-Sheng Chai[a*], Yu-Wei Chang[b], Pai-Ying Luo[c], Tsung-Han Lee[d], Lin-Yu Wu[d], Chiun-Hsun Chen[d]
[ab]Department of Air Transport Industry, Aletheia University, No.32, Zhenli St., Danshui Dist., New Taipei City 25103, Taiwan R.O.C.
[c]Department of Finance and Tax Planning, Aletheia University, No.32, Zhenli St., Danshui Dist., New Taipei City 25103, Taiwan R.O.C.
[d]Department of Mechanical Engineering, National Chiao Tung University 1001 University Road, Hsinchu, Taiwan 300, ROC
**Corresponding author*

ABSTRACT
This study tested a 30 kW-generator in a small biogas plant at the Taiwan Sugar Swine Farm in Taichung. After the desulfurization process, the biogas still contains water vapor. Hence, it is necessary to remove the water vapor from the intake biogas before it is fueled into the engine. In this study, the water vapor in the intake biogas was already removed. In addition, the composition of the intake biogas was identified and concentrations were measured to provide real data. Moreover, a complete ignition system was installed, consisting of a spark-plug pressure sensor and a rotary encoder, to record the in-cylinder pressure and crank angle of the piston cylinder.
In this study, the optimum spark timing of the engine was located at 13 degrees before top-dead center (BTDC13), which supplied the highest power generation. Delaying or advancing the optimum spark timing leads to poorer power outputs. The spark timing of BTDC13 has a lower coefficient of variation in indicated mean effective pressure (CoV_{IMEP}) than delayed and advanced timings, where the engine performs at more stable indicated mean effective pressures (IMEP) during combustion. In addition, it was found that the lower CoV_{IMEP} results in a higher CH_4 consumption ratio.
Keywords: *Biogas generation, Spark timing, Combustion stability*

Date of Submission: 25-08-2026 Date of acceptance: 05-09-2026

I. Introduction

Global warming and the energy shortage crisis are currently serious problems for human beings. Animal manure from farms can produce biogas after anaerobic treatment. The manure and urine of swine includes methane (CH_4), carbon dioxide (CO_2) and nitrous dioxide (NO_x). These gases turn into biogas after anaerobic treatment, which is composed of methane (CH_4) and carbon dioxide (CO_2) with small amounts of hydrogen (H_2), nitrogen (N_2), ammonia (NH_3), hydrogen sulfide (H_2S) and organic compounds. The methane is burnable for generating power and heat.

There are many benefits to using swine manure for making biogas. First, it can reduce greenhouse gas (GHG) emissions. Currently, most governments support the reduction of GHG emissions. The main GHGs in the atmosphere are water vapor, CO_2, CH_4, NO, ozone and chlorofluorocarbons. The global warming potential of methane from untreated animal manure is 23 times that of carbon dioxide. If these gases are emitted to the surroundings, they will have an environmental impact.

Biogas contains water vapor after the desulfurization process, so it is necessary to remove the water vapor from the intake biogas. In addition, details of the intake biogas composition and their concentrations were measured. Moreover, an ignition system was installed in the engine to enhance its performance and combustion stability. After these implementations, the effects of varying the fuel flow rate and the excess air ratio on the engine's performance were studied.

Brown [1] reported that biomass comprises of two-thirds of the total renewable energy in the world. Renewable energy has not yet been fully developed in Taiwan because fossil energy is much cheaper than renewable energy. However, renewable energy will become more competitive in the energy market because Legislative Yuan of Taiwan passed the "Renewable Energy Development Bill" in June 2009, as investigated by

Chen et al. [2]. Moreover, Tsai and Lin [3] surveyed bioenergy from livestock manure management in Taiwan. Based on the characteristics of the swine dung, the benefits from the total swine population from farms (approximately 4.3 million heads) of the farm scale of over 1000-head of swine in Taiwan are as follows: emissions of methane reduced by 21.5 Gg/yr, total electricity generated at 7.2×10^7 kWh/yr, equivalent to a savings in electricity charges of USD7.2×10^6/yr (1 dime per kW-h in Taiwan) and carbon dioxide mitigation of 500 Gg/yr.

Huang [4] used a 73% methane concentration of biogas to compare with 60% CH_4 biogas and applied a heat recovery system to heat the inlet gas under different temperatures and to analyze the preheating influence on the generation performance. The results showed that power generation with 73% CH_4 biogas is higher than the ones with 60% CH_4 biogas, except in the region around $\lambda<0.85$. However, the thermal efficiency increases with increasing methane concentration in the region of $\lambda>0.95$. In the case investigating the effect of increased inlet gas temperature, there is an obvious improvement when the temperature is increased from 40°C to 120°C for a biogas supply rate of 140 L/min with $\lambda=1.58$.

Bika et al. [5] varied H_2 and CO proportions to compare engine knock and combustion characteristics of a spark ignition engine. They found the knock limits (used to determine the safe operating region) and described the knocking characteristics of the fuel in an engine with a spark timing of 12 crank angle degrees before top-dead-center (CAD BTDC). The knock limited equivalence ratio decreases with increasing compression ratio. The non-knocking area falls to the left side of the equivalence ratio versus compression ratio curve.

Arunachalam and Olsen [6] used a CFR F-2 engine fueled with different compositions of manufactured gases to evaluate the knocking characteristics. The critical compression ratio refers to the compression ratio at which the fuel mixture experiences a light audible knock in the test engine. They found that an increase in the volume percentage of CO_2 in the test gas results in an increase in the critical compression ratio. Moreover, there is a decrease in the critical compression ratio as the percentage volume of H_2 in the composition is increased.

Porpatham et al. [7] tested the effect of the CO_2 concentration in biogas on the performance of a constant speed spark ignition engine. A lime water scrubber was used to absorb CO_2 in the biogas. They found that when CO_2 in the biogas is reduced from 41% to 30%, the engine performance is improved by 20%, unburnt hydrocarbons are reduced and the lean limit of combustion is extended.

Park et al. [8] operated an 8-L, 6-cylinder spark ignition engine fueled by various the proportions of methane and nitrogen. The experiment also applied different concentrations of H_2 in biogas at stoichiometric ($\lambda=1$) and lean conditions. The engine operation at $\lambda=1$ with more than 5% H_2 addition makes the decrease of thermal efficiency caused by increasing cooling loss.

Badr et al. [9] carried out a parametric study on the lean misfiring and knocking limits of gas-fueled spark ignition engine. They tested Ricardo E6 engine, using propane and liquefied petroleum gas (LPG) as fuels. For low engine speeds, when the intake temperature increases, the lean misfire limit decreases. For high speeds, when the intake air temperature is up to 70°C, the lean misfire limit increases, however, beyond 70°C the lean misfire decreases.

Biogas generated from the anaerobic treatment of wastewater in a swine farm is a kind of natural renewable energy source. This study developed the ignition system on a biogas generator to enhance its performance and combustion stability. The effects of varying the fuel flow rate and the excess air ratio on the engine's performance are investigated.

II. Experimental Apparatus

2.1 Experiment layout

The experimental equipment layout is shown in Fig. 1. When the engine is running, air and biogas are sucked into the engine automatically. The water vapor in the biogas is removed by a GTT RD15 dehumidifier with a maximum inlet biogas flow rate of 30 L/sec (marked by D) before biogas flows through the flow meter (F1). The flow meters (marked by F1 and F2) measure the air and the biogas flow rates, respectively, and are controlled by valves at the engine inlets. The airflow meter at the air inlet was an insertion-type VA-400 flow sensor with a range that varied with the installed pipe diameter. The measurement range of the flow sensor was 9 – 2700 m^3/h, with an accuracy of approximately ± 3% of the measured value. The biogas flow meter at the biogas inlet was a TF-4130-32 thermal-mass flow meter. The measurement range of the flow sensor was 0 – 500 NL/min, with an accuracy of approximately ± 2% of the measured value.

The crank angle degree is recorded by a HONTKO HPN6A rotary encoder (marked by R). The spark timing controller (marked by ST) can adjust spark timing according to the corresponding crank angle degree. The in-cylinder pressure can be obtained at each crank angle degree by the spark-plug pressure sensor (marked by P), which is modified from an NGK BKR5E-11 spark plug with a PCB Piezotronics 112A05 pressure sensor. The pressure range is up to 350 bar, and the operating temperature ranges from 240 to 310°C. The engine is powered by combustion to drive the generator and produce electricity. A waste gas analyzer, BACHARACH

ECA 450, is placed at the engine outlet to measure the composition of waste gases. This analyzer measured the concentration of oxygen and carbon monoxide and then used that data to deduce the concentration of carbon dioxide. The measurement range of the gas analyzer was 0 – 25% for O_2, 0 – 10% for CO, and 0 – 20% for CO_2, each with an accuracy of approximately ± 0.2% and a resolution of 0.1%.

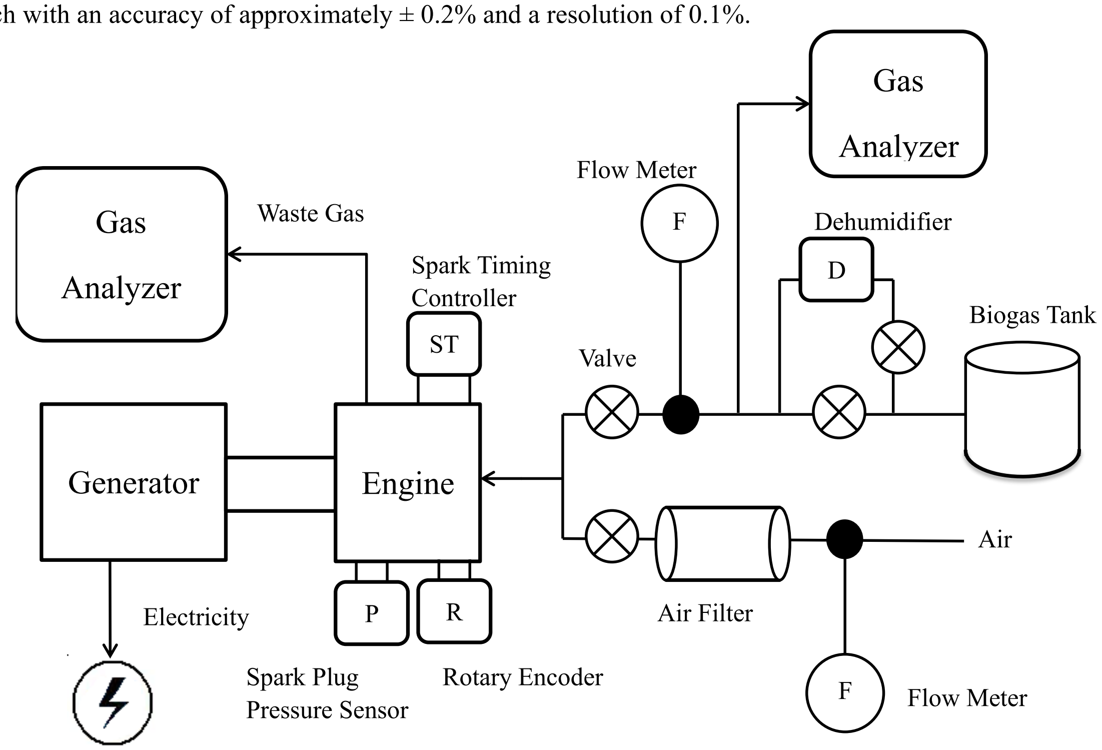

Fig. 1 Experimental Equipment Layout

2.2 The Effect of Spark Timing

The experimental parameters are spark-timing, biogas flow rate and excess air ratio. The biogas flow rates are 220, 240 and 260 L/min, and excess air ratios range from 0.8 to 1.2. The optimum spark timing is adjusted in this study. In addition, the advance and delay of the optimum spark timing are investigated. At each specific spark timing, this study tests different biogas flow rates and each flow rate is accompanied by different excess air ratios.

III. Theoretical Calculations

3.1 Excess Air Ratio

The air-fuel ratio *(AF)* is defined as the ratio of moles of air to fuel in the combustion process. The composition of biogas in this study contains air from the atmosphere, which leaks into the storage tank when the water line of the anaerobic fermentation pool is too low. Hence, the stoichiometric reaction for combustion of biogas with standard air is given as:

$$CH_4 + xCO_2 + y(O_2 + 3.76N_2) + zH_2O + (2-y)(O_2 + 3.76N_2) \rightarrow (1+x)CO_2 + (z+2)H_2O + 7.52N_2 \quad (1)$$

where x, y and z are the moles of CO_2, air and water vapor in the biogas, respectively. Both x and y can be measured by instruments, and z can be obtained from the absoulate humidity of biogas.

The stoichiometric air-fuel ratio, AF_{stoich}, is calculated by:

$$AF_{stoich} = \frac{mole\ of\ air}{mole\ of\ CH_4 + mole\ of\ CO_2 + mole\ of\ air\ in\ biogas + mole\ of\ H_2O}$$

$$= \frac{(2-y)\times 4.76 mole}{(1+x+y\times 4.76+z) mole} \quad (2)$$

AF_{act} can be expressed as:

$$AF_{act} = \frac{Air\ flow\ rate}{Biogas\ flow\ rate} \tag{3}$$

The *Excess Air Ratio (λ)* is the ratio of actual moles of air used to the stoichiometric moles of air, defined as:

$$\lambda = \frac{(mole\ of\ air)_{act}}{(mole\ of\ air)_{stoich}} = \frac{(\frac{mole\ of\ air}{mole\ of\ fuel})_{act}}{(\frac{mole\ of\ air}{mole\ of\ fuel})_{stoich}} = \frac{AF_{act}}{AF_{stoich}} \tag{4}$$

3.2 Consumption of CH_4

The theoretical consumed percentage of CH_4 in waste gas of the combustion process is calculated as follows: The balanced reaction is:

$$CH_4 + xCO_2 + y(O_2 + 3.76N_2) + zH_2O + \lambda(2-y)(O_2 + 3.76N_2) \rightarrow aO_2 + bCH_4 + (2+z-2b)H_2O + (1+x-b)CO_2 + 3.76(y - \lambda y + 2\lambda)N_2 \tag{5}$$

where the NO_x and CO concentrations (on the order of ppm) in waste gas can be neglected. x, y and z are the moles of CO_2, moles of air and moles of water vapor in the biogas, respectively. a and b are the moles of O_2 and CH_4, respectively, in waste gas. a can be calculated from the percent of O_2 in waste gas as follows:

$$Mole\ Fraction\ of\ O_2(\%) = \frac{a}{1+x+4.76(y-\lambda y+2\lambda)+z} \tag{6}$$

where $1 + x + 4.76(y - \lambda y + 2\lambda) + z$ is the total moles in waste gas, and b is obtained from the atom balance as:

$$b = 1 - \lambda + \frac{a-y+\lambda y}{2} \tag{7}$$

The theoretical percent of used CH_4 is defined as:

$$Theoretical\ Percentage\ of\ Consumed\ CH_4(\%) = \frac{(CH_4)_{in} - (CH_4)_{out}}{(CH_4)_{in}} \tag{8}$$

3.3 Combustion Stability

The *combustion stability*, the coefficient of variation in indicated mean effective pressure (CoV_{IMEP}), is defined as:

$$Combustion\ Stability(CoV_{IMEP}) = \frac{\sigma_{IMEP}}{\overline{IMEP}} \times 100\% \tag{9}$$

where $IMEP$ is the indicated mean effective pressure, which is calculated by integrating pressure with respect to the response volume during the combustion process, and V_d is the effective working volume. $\overline{IMEP}$ is the average of $IMEP$. σ_{IMEP} is the standard deviation of $IMEP$. Their formulations are as following:

$$Indicated\ Mean\ Effect\ Pressure\ (IMEP) = \frac{1}{V_d}\int PdV \tag{10}$$

$$\overline{IMEP} = \frac{1}{n}\sum_{k=1}^{n}(IMEP)_k \tag{11}$$

$$\sigma_{IMEP} = \sqrt{\frac{1}{n}\sum_{k=1}^{n}[(IMEP)_k - \overline{IMEP}]^2} \tag{12}$$

where n is the number of combustion cycles.

IV. Results and Discussion

The biogas used in this research was supplied from an anaerobic tank made of a red plastic bag. The H_2S concentration in the biogas was effectively reduced from 4000 ppm to 50 ppm after the H_2S removal system. The detailed composition of the biogas is as follows: 69% CH_4, 13.3% CO_2, 12.38% air, 1.99% H_2O and 3.33% residues. The biogas containing air and water vapor is previously dehumidified before it is sucked into the engine. The intake temperature of the biogas is 27°C with a relative humidity of 53%.

4.1 Power Generation

The power outputs with different excess air ratios are shown in Figs. 2a~c for the different spark timings. The excess air ratio for a 260 L/min biogas supply rate cannot reach 1.0 because the limit of the maximum allowable total volume flow rate into the engine is 2000 L/min. There is a drop on the fuel rich side, except with the biogas supply rate of 240 L/min with a spark timing of BTDC9, whose peak is located at λ=0.9. Note that the biogas supply rate of 260 L/min with a spark timing of BTDC9 provides a better power output than BTDC17; as the biogas supply rate decreases, the spark timing of BTDC17 indicates greater power output than BTDC9. There are two factors, the density of the gas mixture and the burning angle that can affect the relationship between the biogas supply rate and spark timing. The advanced spark timing has a longer overall burning process time, but the delayed spark timing provides a smaller burning angle due to the exhaust valve opening. In contrast, the delayed spark timing supplies a higher density of gas mixture, but the density of the gas mixture with advanced spark timing is smaller due to the longer stroke. Thus, the effect of the gas mixture density is larger than the effect of the burning angle when the biogas supply rate is 260 L/min. As the biogas supply rate decreases, the effect of the burning angle is more obvious than the effect of the gas mixture density.

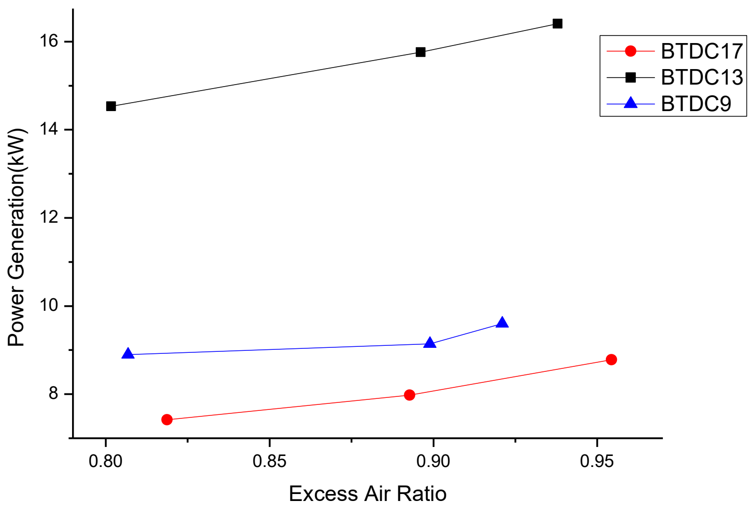

Fig. 2a Power generation v.s. excess air ratio with 260L/min biogas supply and different spark timings

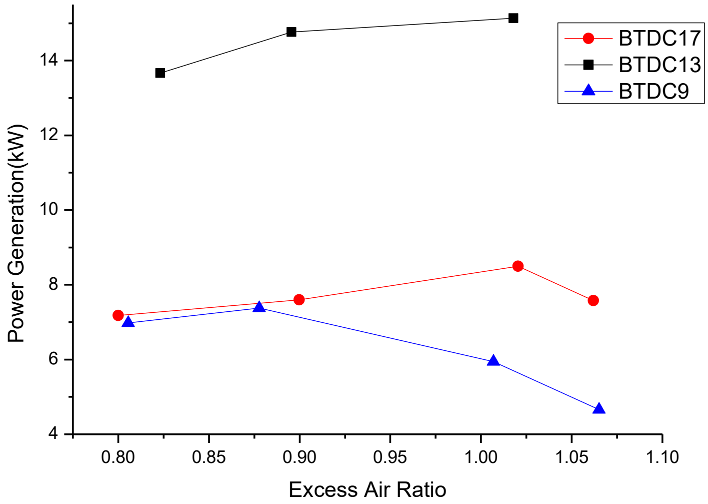

Fig. 2b Power generation v.s. excess air ratio with 240L/min biogas supply and different spark timings

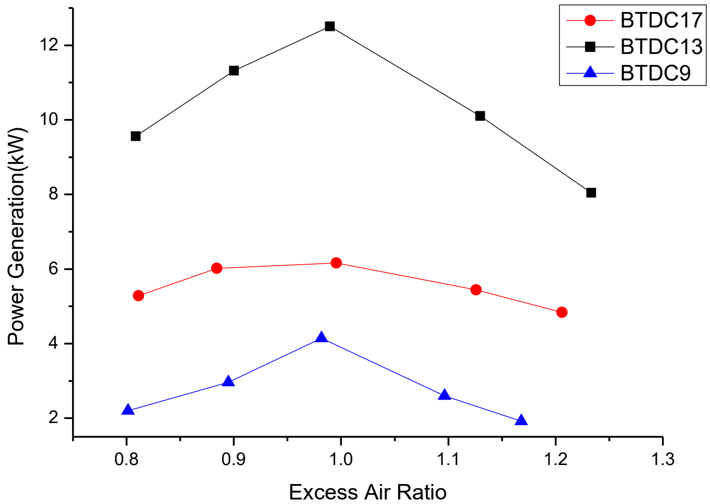

Fig. 2c Power generation v.s. excess air ratio with 220L/min biogas supply and different spark timings

In addition, both the faster and slower spark timings than the optimum spark timing of BDTC13 lead to a decrease in power output. This is because the gas mixture (intake biogas and intake air) are not pushed into the proper position in the piston to ignite. The work transfer from the piston to the gas mixture in the cylinder at the end of the compression stroke is too large if combustion starts too early in the cycle. This results in the auto-ignition of the unburnt gas mixture due to the heat radiation from the flame front of the spark plug. In contrast, if the spark timing starts too late, the peak in-cylinder pressure is reduced and the expansion stroke (where work transfers from the gas mixture to the piston) decreases.

4.2 Waste Gas Analysis

The waste gas temperatures for the different spark timings and biogas supply rates as a function of excess air ratio are shown in Fig. 3. The figure reveals that the maximum temperature occurs around the stoichiometric point (λ=0.9~1.0) and that it is decreasing toward the fuel-rich and fuel-lean regions for each spark timing. Furthermore, the exhaust temperature is also affected by different spark timings. Delaying spark timing, as in BTDC9, from the optimum value increases waste gas temperature. This is because the volume of the combustion chamber is smaller at the slower spark timing, so it decreases the heat losses to the combustion chamber wall. In contrast, the waste gas loses abundant heat through the combustion chamber if the spark timing is advanced. Therefore, the waste gas temperature is lower than the others due to the heat losses.

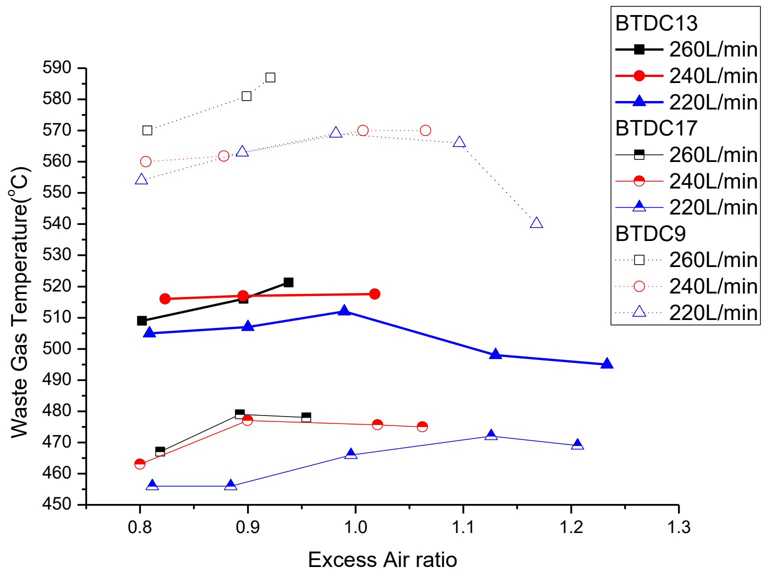

Fig. 3 Waste gas temperature v.s. excess air ratio with different biogas supply and different spark timings

Figs. 4a~c show the estimated CH_4 consumption ratios as a function of the excess air ratio with different biogas supplies and different spark timings. It can be observed that the maximum consumption ratio occurs at approximately the stoichiometric condition ($0.9<\lambda<1.1$), and then it decreases toward both the fuel-rich and fuel-lean regions. In addition, the CH_4 consumption ratio is higher when the engine operates at optimal spark timing with a fixed biogas flow supply. In comparison with the advanced spark timing, the delayed spark timing achieves higher CH_4 consumption ratios.

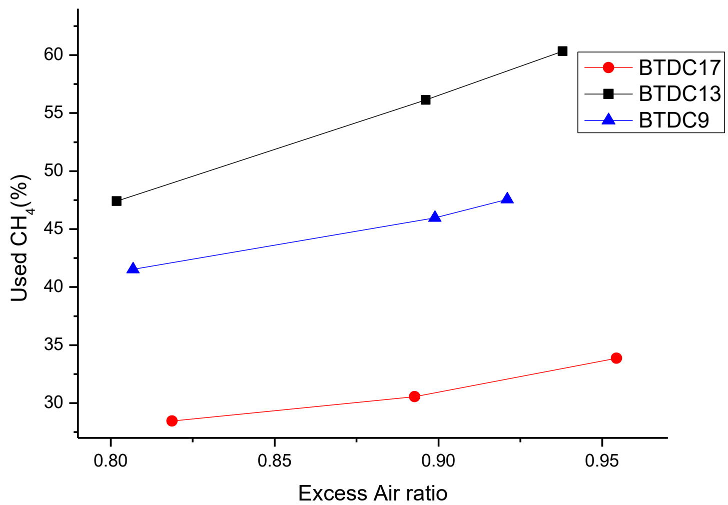

Fig. 4a Estimated CH_4 consumption ratios v.s. excess air ratio with 260L/min biogas supply and different spark timings

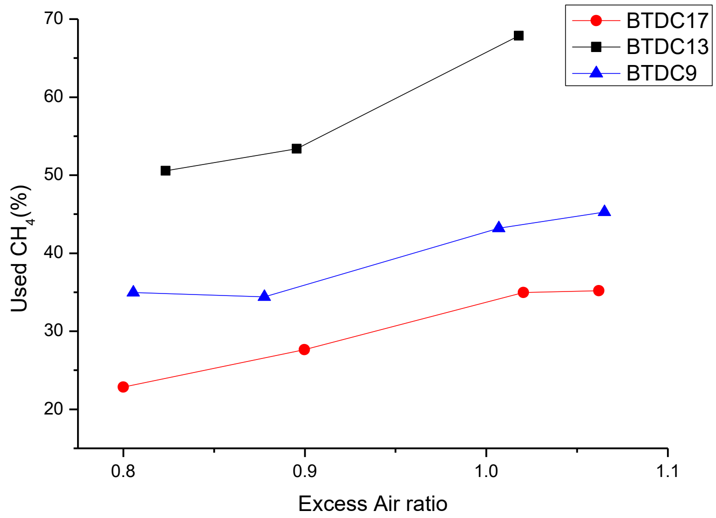

Fig. 4b Estimated CH_4 consumption ratios v.s. excess air ratio with 240L/min biogas supply and different spark timings

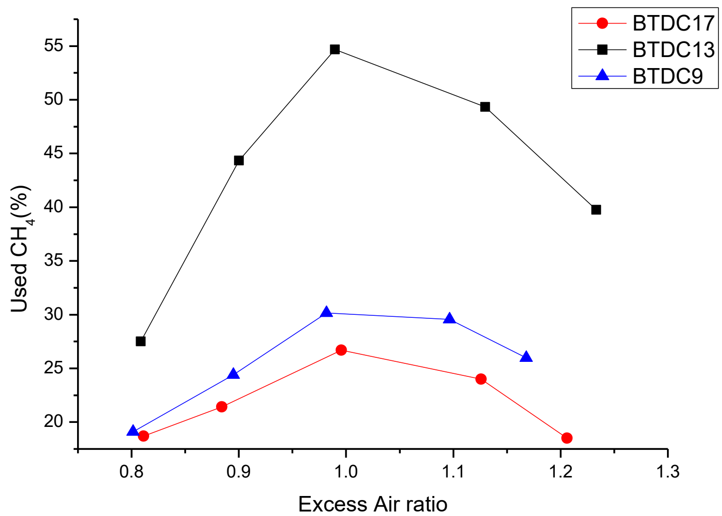

Fig. 4c Estimated CH_4 consumption ratios v.s. excess air ratio with 220L/min biogas supply and different spark timings

4.3 In-cylinder Pressure Analysis

Figure 5 and 6 show the pressure of cylinder as crank angle and volume with different spark timing. It can find that the spark timing of the maximum pressure is BTDC17. Because the ignition delay is increased, the pressure of increased rate is higher in the premixed combustion stage to lead to higher pressure. However, the spark timings of BTDC17 and BTDC9 are unstable and lead to knock, because they are not the optimized spark timing. When the spark timing is advanced or delayed, the mix gas into the cylinder will not burn completely in the spark timing. When the unburned gas will be fired to at another time, knock is occurred.

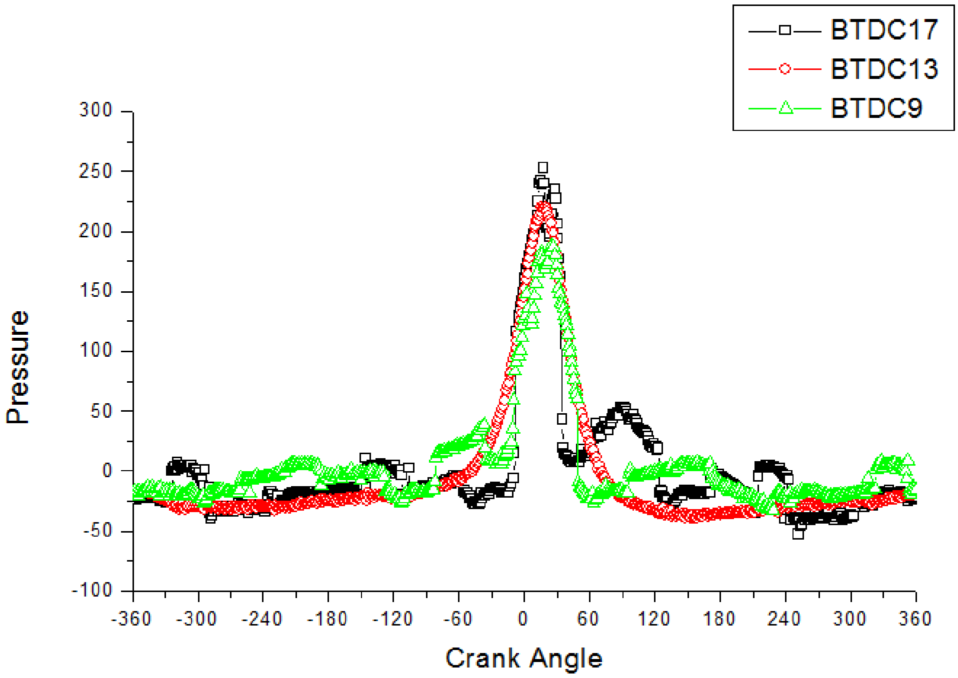

Fig.5 Pressure v.s. crank angle with different spark timing

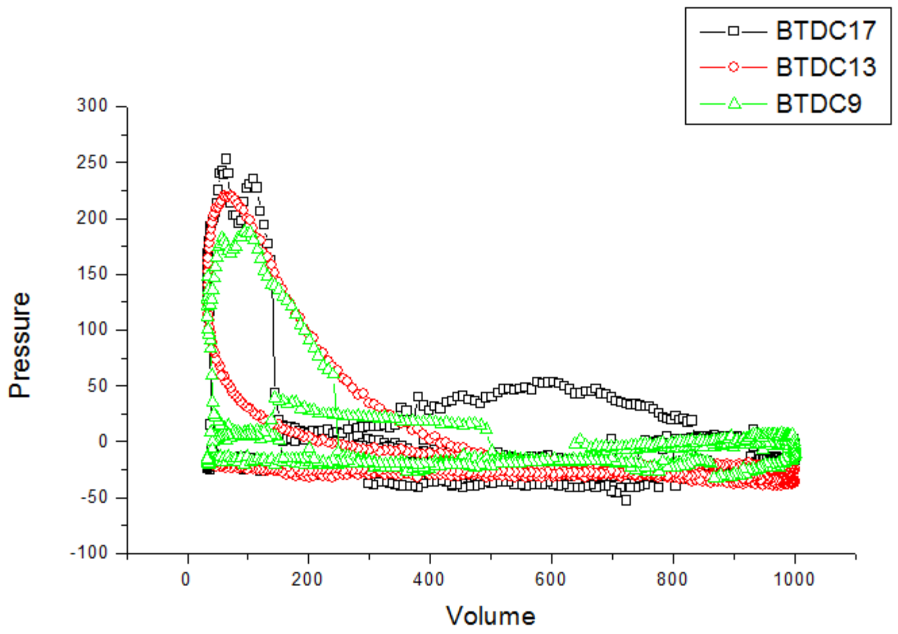

Fig.6 Pressure v.s. Volume with different spark timing

The combustion stability (CoV_{IMEP}) is calculated by the measured combustion pressure during 200 consecutive cycles. It is found that the spark timing for maximum power output is 13 degree (BTDC13) before top-dead-center. Figs. 7a~c show the CoV_{IMEP} as a function of the excess air ratio with different biogas supply rates and different spark timings. It can be observed from these figures that CoV_{IMEP} has a minimum value near the stoichiometric point, where the engine achieves a more stable IMEP during combustion with a higher work output, and it increases toward fuel-rich and fuel-lean regions. When the engine is operated in the fuel-rich or fuel-lean region, the fluctuations of in-cylinder pressure become unsteady during the combustion process. The CoV_{IMEP} is also affected by the spark timing. The spark timing of BTDC13 provides a lower CoV_{IMEP} than the advanced and delayed spark timing with the biogas supply rates of 220, 240 and 260 L/min. Thus, the cycle-by-cycle in-cylinder pressure variations of spark timing BTDC13 are smaller than the other two spark timings. The CoV_{IMEP} of delayed spark timing shows a lower performance than that of the advanced one because the self-ignition of the unburnt gas mixture may occur at the advanced spark timing. If combustion starts too early in the cycle, it will result in the work transferring from the piston to the gas mixture in the cylinder at the end of the compression stroke being too large. This causes auto-ignition of the unburnt gas mixture due to heat radiation from the flame front of the spark plug. The in-cylinder pressure fluctuates severely because two flames develop in the cylinder at the same time. Moreover, the advanced spark timing makes the knock of the engine more likely. The knock originates with the extremely rapid release of abundant energy contained in the end-gas before the propagating flame, leading to a high local pressure. Such pressure generates shock waves that propagate through the cylinder and may weaken the materials and cause resonance of the cylinder at its natural frequency.

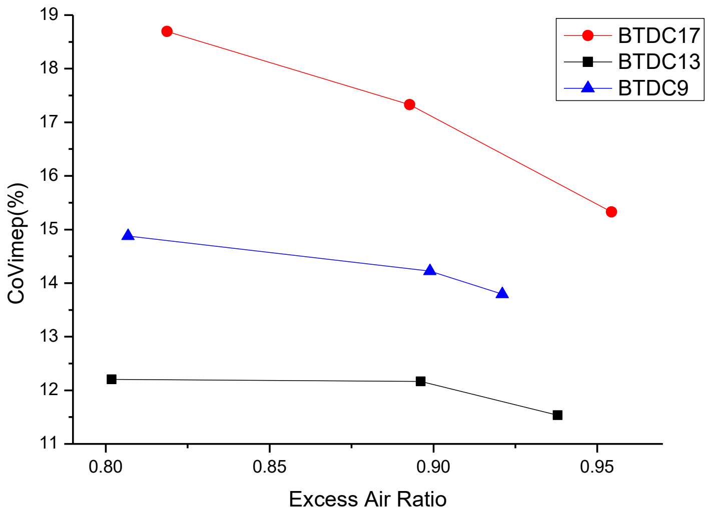

Fig. 7a CoV$_{\mathrm{IMEP}}$ v.s. excess air ratio with 260L/min biogas supply and different spark timings

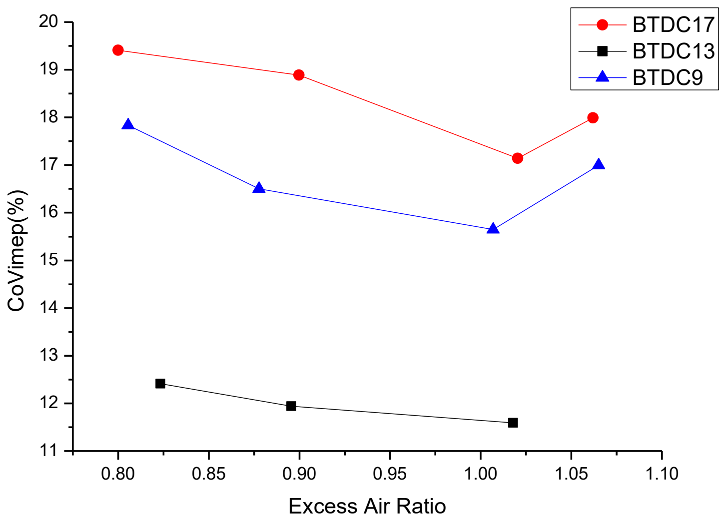

Fig. 7b CoV$_{\mathrm{IMEP}}$ v.s. excess air ratio with 240L/min biogas supply and different spark timings

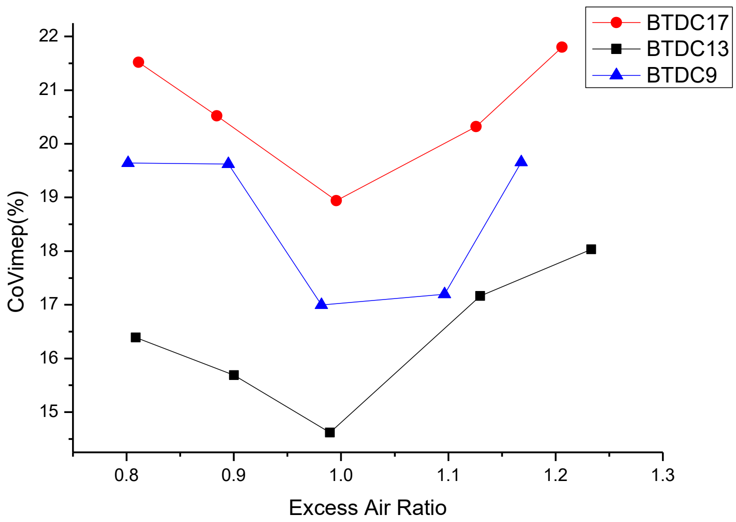

Fig. 7c CoV_{IMEP} v.s. excess air ratio with 220L/min biogas supply and different spark timings

From Figs. 4a~c and Figs. 7a~c, it can be observed that there are opposite trends between the CoV_{IMEP} and the estimated CH_4 consumption ratio. The relationship between the CoV_{IMEP} and the estimated CH_4 consumption ratio under different spark timings is shown in Fig. 8. The figure reveals that at lower CoV_{IMEP}, the in-cylinder pressure fluctuates more, resulting in a higher CH_4 consumption ratio.

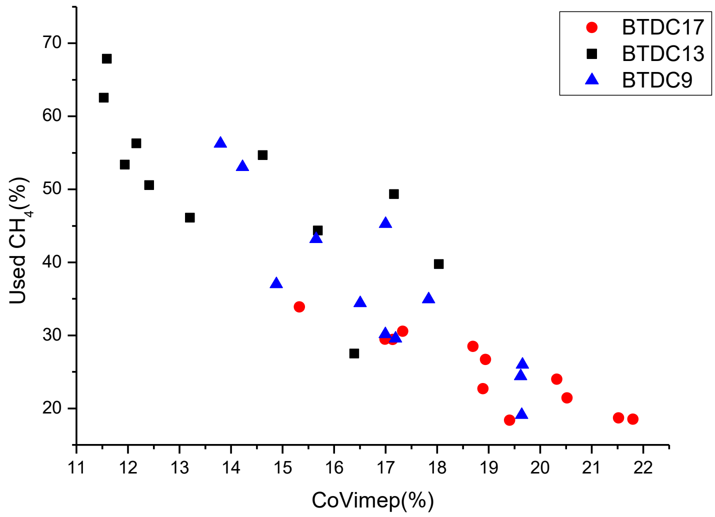

Fig. 9 Estimated CH_4 consumption ratios v.s. CoV_{IMEP} with different spark timings

V. Conclusions

According to the experimental results, the following conclusions can be drawn from this study:

- The optimum spark timing of the present engine is located at BTDC13, where it supplies a larger power output than other spark timings. At a given biogas supply rate and excess air ratio, the power generation, and percentage of used CH_4 are highest when operating at the spark timing of BTDC13.
- The delayed spark timing of BTDC9 leads to a higher exhaust gas temperature and reduces the NO_x emission at a given biogas supply rate.
- For a given biogas supply rate, the spark timing of BTDC13 has the lowest CoV_{IMEP}, and the BTDC17 has the largest CoV_{IMEP}. There is an opposite trend between the CoV_{IMEP} and CH_4 consumption ratio, which indicates that the lower CoV_{IMEP} causes the higher CH_4 consumption ratio.

Acknowledgements
The authors express their grateful appreciation to the Ministry of Science and Technology for their financial support under the projects MOST 104-3113-E-009-001.

References

[1] A. Brown, 2010 Survey of Energy Resources, World Energy Council, London, 2010.
[2] Falin Chen, Shyi-Min Lu , Eric Wang, Kuo-Tung Tseng, Renewable energy in Taiwan, Renewable and Sustainable Energy Reviews, 14 (2010) 2029-2038.
[3] Wen-Tien Tsai, Che-I Lin, Overview analysis of bioenergy from livestock manure management in Taiwan, Renewable and Sustainable Energy Reviews, 13 (2009) 2682-2688.
[4] Tsung-Han Lee, Sheng-Rung Huang, Chiun-Hsun Chen, The experimental study on biogas power generation enhanced by using waste heat to preheat inlet gases, Renewable Energy, 50 (2013) 342-347.
[5] Anil Singh Bika, Luke Franklin, David B. Kittelson, Engine knock and combustion characteristics of a spark ignition engine operating with varying hydrogen and carbon monoxide proportions, Hydrogen Energy, 36 (2011) 5143-5152,.
[6] Aparna Arunachalam, Daniel B. Olsen, Experimental evaluation of knock characteristics o producer gas, Biomass and Bioenergy, 37 (2012) 169-176.
[7] E. Porpatham, A. Ramesh, B. Nagalingam, Investigation on the effect of concentration of methane in biogas when used as a fuel for a spark ignition engine, Fuel, 87 (2008) 1651−1659.
[8] O. Badr, N. Alsayed and M. Manaf, "A parametric study on the lean misfiring and knocking limits of gas-fueled spark ignition engines",18,pp.579-594,1998.
[9] Cheolwoong Park, Seunghyun Park, Yonggyu Lee, Changgi Kim, Sunyoup Lee, Yasuo Moriyoshi, "Performance and emission characteristics of a SI engine fueled by low calorific biogas blended with hydrogen" , Hydrogen Energy, 36, pp.10080-10088, 2011.